Biochemical and Biophysical Research Communications 374 (2008) 111–116

Contents lists available at ScienceDirect

Biochemical and Biophysical Research Communications

journal homepage: www.elsevier.com/locate/ybbrc

# Blocking CD147 induces cell death in cancer cells through impairment of glycolytic energy metabolism

Miyako Baba [a,*], Masahiro Inoue [b], Kazuyuki Itoh [c], Yasuko Nishizawa [a]

[a] Department of Pathology, Osaka Medical Center for Cancer and Cardiovascular Diseases, Research Institute, 1-3-2 Nakamichi, Higashinari-ku, Osaka 537-8511, Japan
[b] Department of Tumor Biochemistry, Osaka Medical Center for Cancer and Cardiovascular Diseases, Research Institute, Higashinari-ku, Osaka, Japan
[c] Department of Biology, Osaka Medical Center for Cancer and Cardiovascular Diseases, Research Institute, Higashinari-ku, Osaka, Japan

ARTICLE INFO

*Article history:*
Received 19 June 2008
Available online 9 July 2008

*Keywords:*
CD147
Cell death
MCT-1
Acidosis
Glycolytic energy metabolism

ABSTRACT

CD147 is a multifunctional transmembrane protein and promotes cancer progression. We found that the anti-human CD147 mouse monoclonal antibody MEM-M6/1 strongly induces necrosis-like cell death in LoVo, HT-29, WiDr, and SW620 colon cancer cells and A2058 melanoma cells, but not in WI-38 and TIG-113 normal fibroblasts. Silencing or overexpression of CD147 in LoVo cells enhanced or decreased the MEM-M6/1 induced cell death, respectively. CD147 is known to form complex with proton-linked monocarboxylate transporters (MCTs), which is critical for lactate transport and intracellular pH (pHi) homeostasis. In LoVo cells, CD147 and MCT-1 co-localized on the cell surface, and MEM-M6/1 inhibited the association of these molecules. MEM-M6/1 inhibited lactate uptake, lactate release, and reduced pHi. Further, the induction of acidification was parallel to the decrease of the glycolytic flux and intracellular ATP levels. These effects were not found in the normal fibroblasts. As cancer cells depend on glycolysis for their energy production, CD147 inhibition might induce cell death specific to cancer cells.



Tumor cells mainly depend on anaerobic glycolysis for production of ATP even in the presence of oxygen, in contrast to normal tissues such as brain, heart and red skeletal muscle, which depend on mitochondrial respiration [1,2]. As accumulation of lactate, the end product of anaerobic glycolysis, causes acidosis in the cells, it is critical for cancer cells to pump out lactate across the plasma membrane. The pHi homeostasis has recently shown to be a novel therapeutic target, as suppression of proton-linked monocarboxylate transporters (MCT-1 and -2 expression) was shown to induce necrosis in malignant glioma cells through accumulation of lactate and a decrease of pHi [3]. MCTs are non-glycosylated multispan proteins with 12 predicted transmembrane domains and cytoplasmic N- and C-terminal ends. Of the 14 known family members, MCT-1, -2, -3, and -4 have proton-linked monocarboxylate transport kinetics [4]. Lactate transport across the plasma membrane by these MCTs is essential for maintenance of intracellular pH (pHi) homeostasis [4–7].

CD147 (also known as extracellular matrix metalloproteinase inducer, basigin, neurotelin) is a multifunctional transmembrane protein with two extracellular Ig-like domains and a cytoplasmic tail of 40 amino acids [8]. CD147 is ubiquitously expressed on cell surface, with the highest levels found in metabolically active cells such as lymphoblasts and malignant tumor cells [9,10]. The protein promotes proliferation and metastasis of cancer cells through increasing production of hyaluronan [11], and stimulating the production of multiple matrix metalloproteinases (MMPs) by fibroblasts, endothelial cells and tumors cells and the activation of VEGF-A by MMPs [12–15]. CD147 is also involved in intracellular lactate homeostasis by associating with MCT-1 and MCT-4, caring sorting information for polarized targeting of the MCT-1/CD147 hetero-complexes, and facilitating MCT expression on the cell surface of normal and cancer cells [5–7]. Therefore, we speculated that impairment of CD147 causes cell death for cancer cells by disturbing monocarboxylate transport and consequent pHi homeostasis.

In the present study, we report that an anti-CD147 mouse monoclonal antibody (clone MEM-M6/1) as well as shRNA of CD147 strongly induces necrosis-like cell death in several colon cancer cells including LoVo cells and melanoma cells, but not in normal fibroblasts. We investigated the association between CD147, MCT-1, and glycolytic energy metabolism in the induction of cell death.

## Materials and methods

*Cell culture.* LoVo and WiDr colon cancer cells, A2058 melanoma cells, and WI-38 and TIG-113 cells were obtained from the Japan Health Sciences Foundation (Tokyo, Japan), and HT-29 and SW-620 colon cancer cells were obtained from the American Type Culture Collection (Manassas, VA). These cells were cultured in F-12

* Corresponding author. Fax: +81 6 6973 5691.
*E-mail address:* baba-mi@mc.pref.osaka.jp (M. Baba).

0006-291X/$ - see front matter © 2008 Elsevier Inc. All rights reserved.
doi:10.1016/j.bbrc.2008.06.122

Nutrient medium (Invitrogen, Carlsbad, CA) for LoVo cells, Dulbecco's modified Eagle's medium (Invitrogen) for HT-29, WiDr, SW620 and A2058 cells, and Eagle's MEM medium (Invitrogen) supplemented with non-essential amino acids (Invitrogen) for WI-38 and TIG-113 cells. The medium was supplemented with 10% fetal bovine serum (Sigma, St. Louis, MO), penicillin G (50 μg/ml), and streptomycin (50 μg/ml).

*Evaluation of cell death.* The cells were treated with anti-human CD147 mouse monoclonal antibody (clone MEM-M6/1, isotype IgG1, Abcam, Cambridge, UK) and mouse normal IgG1 (Sigma) as a control. Evaluation of cell death was carried out by trypan blue exclusion assay.

*Plasmid construction.* To construct the CD147-EGFP expression vector, CD147 cDNA (GenBank Accession No. AB072923) fragment amplified by RT-PCR was inserted into a pEGFP-N1 vector (Clontech, Mountain View, CA). The shRNA targeting sequences for CD147 (AB072923) and MCT-1 (GenBank Accession No. L31801) were from Xu et al. and Mathupala et al., respectively [3,16]. The shRNA template oligonucleotides were cloned into a pSilencer 3.1-H1 puro vector (Ambion, Austin, TX). The presence of their correct sequences was verified using an ABI PRISM 310 DNA Analyzer (Applied Biosystems, Foster City, CA). The transfection and selection of the CD147-EGFP and shRNA expression vectors were carried out as previously described [17].

*Western blotting.* Cells were lysed using sample buffer and Western blotting was carried out using soluble protein (40 μg), anti-CD147 mouse monoclonal antibody (Abcam) and anti-MCT-1 goat polyclonal antibody (Santa Cruz, Santa Cruz, CA) as described previously [17].

*Real-time PCR.* Real-time PCR with SYBR green was performed using Power SYBR Green PCR Master Mix (Applied Biosystems) and a 7500 Real-Time PCR System (Applied Biosystems). The following primer sets (each 5 pmole) were used to amplify MCT-1 (GenBank Accession No. L31801), and β-actin (GenBank Accession No. X00351) cDNA fragments:

MCT-1 forward primer 5′-TGGGACTTGTAGCCAACACAAA-3′ and reverse primer 5′-ACGGAAGCCGCAAAGAAATA-3′ and
β-actin forward primer 5′-GCGCGGCTACAGCTTCA-3′ and reverse primer 5′-CTTAATGTCACGCACGATTTCC-3′.

*Immunofluorescence.* Cells cultured on poly-L-lysine cover slips (BD Biosciences, Bedford, MA) were fixed and permeabilized. After blocking, the cells were double stained using anti-human CD147 mouse monoclonal antibody (Abcam) and anti-human MCT-1 goat polyclonal antibody (Santa Cruz), following Alexa Fluor 488-labeled anti-mouse IgG (Molecular Probes, Eugen, OR) or Alexa Fluor 594-labeled anti-goat IgG (Molecular Probes), respectively.

*Metabolic analysis.* Lactate uptake was measured according to Kobayashi et al [18]. The cells ($2 \times 10^5$) were cultured on a 24-well microplate for 48 h. After wash with Hepes buffer, cells were pre-incubated at 37 °C for 10 min in the buffer. Uptake was initiated by applying 0.5 ml Hepes buffer containing [U–$^{14}$C] L-lactic acid (0.2 μCi/ml) (MP Biomedicals, Irvine, CA). After incubation at 37 °C for 5 min, the cells were washed with ice-cold Hepes buffer. The cells were then solubilized in 0.5 ml of 1% SDS/0.2 N NaOH and mixed with 8 ml of aquazol II (GE Healthcare Biosciences, Little Cholfont, Buckinghamshire, UK) to measure the radioactivity in a liquid scintillation counter (Wallac 1409 DSA, Perkin Elmer, Wellesley, MA). Data were normalized using protein content of cell lysates.

Intracellular pH (pHi) was measured according to Frank et al [19]. Cells ($1 \times 10^7$ cells/ml) were suspended in Hepes buffer (pH 7.4) and incubated with 0.5 μM 2′,7′-bis-(2-carboxyethyl)-5-(and-6)-carboxyfluorescein acetoxymethyl ester (BCECF-AM) (Molecular Probes) for 15 min at 37 °C. Then the cell suspension ($1 \times 10^6$ cells/tube) was analyzed by flow cytometry (FACSCaliber, BD Biosciences). pHi was determined as the peak FL1/FL2 ratio. Calibration curves were constructed from the peak ratio FL1/FL2 ratio histogram in the pH range 6.4–7.6.

Glycolytic flux was performed according to Marin-Hernandez et al. [20]. Cells (15 mg protein/ml) were incubated in 3 ml Krebs-Ringer medium with orbital stirring at 37 °C in a plastic tube. After 10 min, 5 mM glucose was added to the cells. The reaction was stopped with cold 3% perchloric acid at 0 and 3 min later. L-Lactic acid generated for 3 min was determined using Enzymatic BioAnalysis (Roche, Darmstadt, Germany).

Cellular ATP levels were determined with a cellular ATP assay kit containing luciferase reagent and cell lysis reagent (Cellular ATP Assay kit, Toyo Ink, Tokyo, Japan) according to the manufacture's protocol.

*Statistical analysis.* Data were expressed as mean ± standard error variance. Between-group statistical differences were determined by applying the Student's $t$ test. $p < 0.05$ was considered as significant.

## Results

### *Anti-CD147 antibody induced cell death in cancer cells*

LoVo colon cancer cells were cultured for 8 days with the anti-CD147 antibody, MEM-M6/1. When the cell growth reached about 50% confluence, cell viability rapidly decreased and strong induction of cell death began. Normal mouse IgG did not influence cell viability at all (Fig. 1A). The MEM-M6/1-induced cell death was dose-dependent over a range of 1.25–10 μg/ml (Supplementary Fig. 1). In addition, HT-29, WiDr and SW620 colon cancer cells and A2058 melanoma cells also underwent cell death in the presence of MEM-M6/1 as well as LoVo cells. Meanwhile, the effect did not occur in WI-38 and TIG-113 normal fibroblasts (Fig. 1B), suggesting that cell death induced by MEM-M6/1 is cancer cell-specific.

### *Characterization of MEM-M6/1-induced cell death*

We examined the mode of cell death in LoVo cells induced by MEM-M6/1. Morphologically, neither chromatin condensation nor nuclear fragmentation, the hallmarks of apoptosis, was observed (Fig. 1C). In addition, the activities of caspase-3 and -8 did not increase in the lysates 24 and 48 h after addition of MEM-M6/1 (Supplementary Fig. 2). These results indicate that the mode of cell death induced by MEM-M6/1 was not apoptosis but necrosis-like. Cell death induced by MEM-M6/1 in other cancer cells examined above was similar to that observed in LoVo cells (data not shown).

### *Critical role of CD147 in MEM-M6/1-induced cell death*

To clarify the direct contribution of CD147 to MEM-M6/1-induced cell death, CD147 expression was suppressed in LoVo cells by CD147 shRNA vector. The CD147 levels in LoVo cells stably expressing CD147 shRNA decreased by approximately 50% relative to mock-transfected cells (Fig. 2A). The CD147 knockdown cells showed accelerated cell death in the presence of MEM-M6/1 compared to control cells (Fig. 2B). In addition, when CD147 was overexpressed in LoVo cells (Fig. 2C), MEM-M6/1-induced cell death was markedly attenuated (Fig. 2D). These results indicate that loss of CD147 is critical for the cell death induced by MEM-M6/1. Next, we assessed the correlation between CD147 expression levels and sensitivity to MEM-M6/1-induced cell death in various cells. The

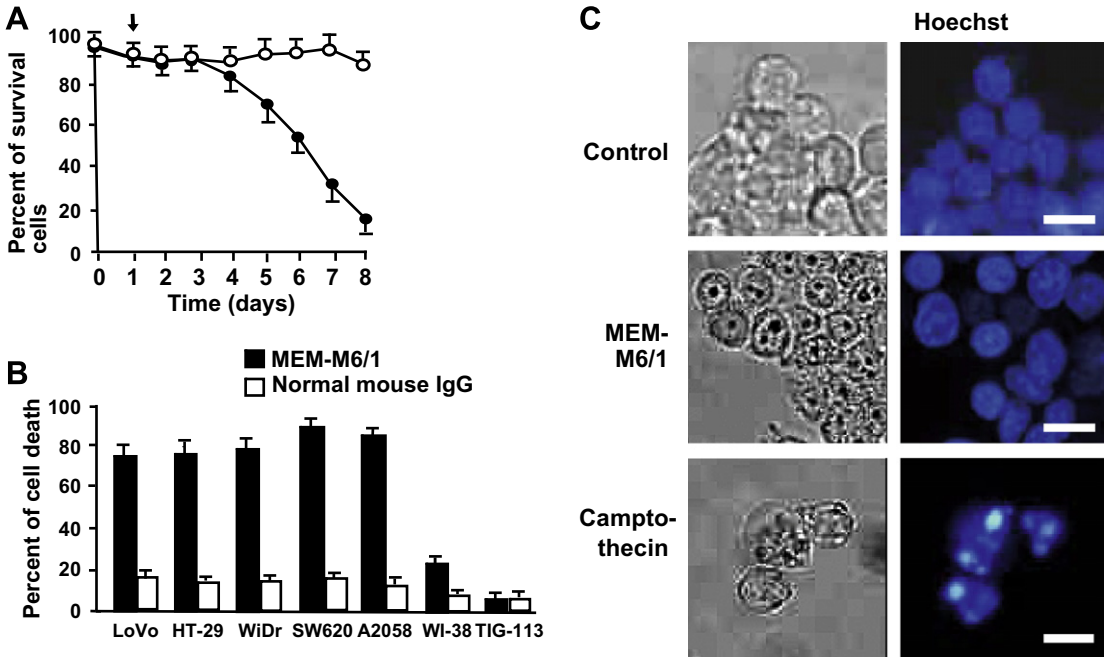


**Fig.1.** LoVo cells ($3 \times 10^4$) were plated on a 24-well microplate. One day later, 5 μg/ml MEM-M6/1 or 5 μg/ml normal mouse IgG (as control) was added to the medium (arrows) and cultured for 8 days. The medium with the same concentration of the antibodies was changed every three days. Percent of survival cells over time is shown in (A). Colon cancer cells, LoVo, HT-29, WiDr or SW620, A2058 melanoma cells, or normal fibroblasts, WI-38 or TIG-113, were plated on a 24-well microplate, $1 \times 10^5$ cells per well. At 50% confluence, 2.5 μg/ml MEM-M6/1 was added to the medium. Percent of cell death after incubation for 72 h is shown in (B). Each value represents mean ± SE from triplicate experiments (A,B). LoVo cells were cultured with 2.5 μg/ml MEM-M6/1 for 72 h and stained with 1 μg/ml Hoechst 33342 at 37 °C for 10 min and observed by fluorescence microscopy (Nikon, Tokyo, Japan) (C). Bar = 20 μm.

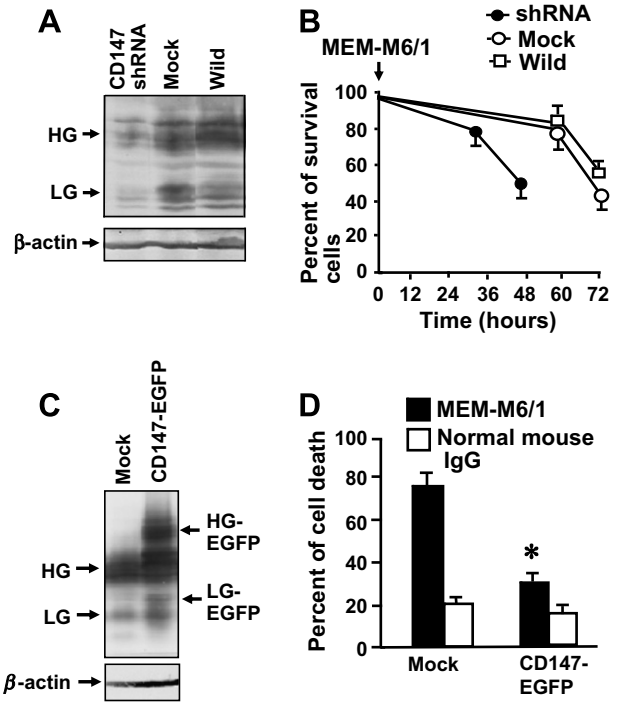


**Fig. 2.** Western blotting of CD147 for shRNA/CD147 (A) and CD147-EGFP (C) transfected cells. Both highly glycosylated (HG) CD147 and less glycosylated (LG) CD147 [26] were detected in the blots. Mock and Wild represent empty vector transfected cells, and non transfected cells, respectively. The cells were cultured until about 60% confluence, and then 2.5 μg/ml MEM-M6/1 was added to the medium. The percent of survival cells over time is shown in (B) and the percent of cell death is shown in (D). The experiments were carried out triplicate. $^*p < 0.05$ vs. mock-transfected cells.

MEM-M6/1 sensitive cancer cells expressed higher levels of CD147 than the resistant normal cells with the exception that the MEM-M6/1 sensitive A2058 cells had lower CD147 expression compared to the resistant TIG-113 normal fibroblast (Supplementary Fig. 3). Thus, expression levels of CD147 are not likely to be the sole factor, which determined the MEM-M6/1-induced cell death.

### *MEM-M6/1 inhibited MCT-1 function by blocking formation of CD147/MCT-1 complex*

It was reported that CD147 forms complex with monocarboxylate transporters, MCT-1 and -4, which is essential for MCT activation [6]. The levels of MCT-1 mRNA (Fig. 3A) and protein (Supplementary Fig. 4A) in five cancer cells were markedly higher than those of WI-38 and TIG-113 normal fibroblasts. In contrast, the levels of MCT-4 mRNA showed no significant difference between cancer cells and normal fibroblasts (Supplementary Fig. 4B). In concert with MCT-1 expression, lactate uptake, which indicates MCT activity, was predominantly elevated in all cancer cells compared to normal fibroblasts (Supplementary Fig. 4C). Moreover, the cell death was induced in LoVo cells, 72 h after transfection with MCT-1 shRNA (Fig. 3B).

Next, we examined the effect of MEM-M6/1 on CD147/MCT-1 complex. Immunofluorescence analysis showed that CD147 and MCT-1 co-localized on the cell surface in LoVo cells (Fig. 3C). In the presence of MEM-M6/1 for 36 h, MCT-1 was distributed in the cytoplasm (Fig. 3C). Then, we investigated the effect of MEM-M6/1 on MCT functions in cancer cells. In the MEM-M6/1 treated cells, MCT-1 activity, rates of lactate uptake (Fig. 4A) as well as the levels of lactate release (Supplementary Fig. 5) decreased, and the levels of pHi of MEM-M6/1 treated LoVo cells was significantly lower compared to those of non treated control (Fig. 4B). These results were parallel to those of the MCT-1 knockdown cells

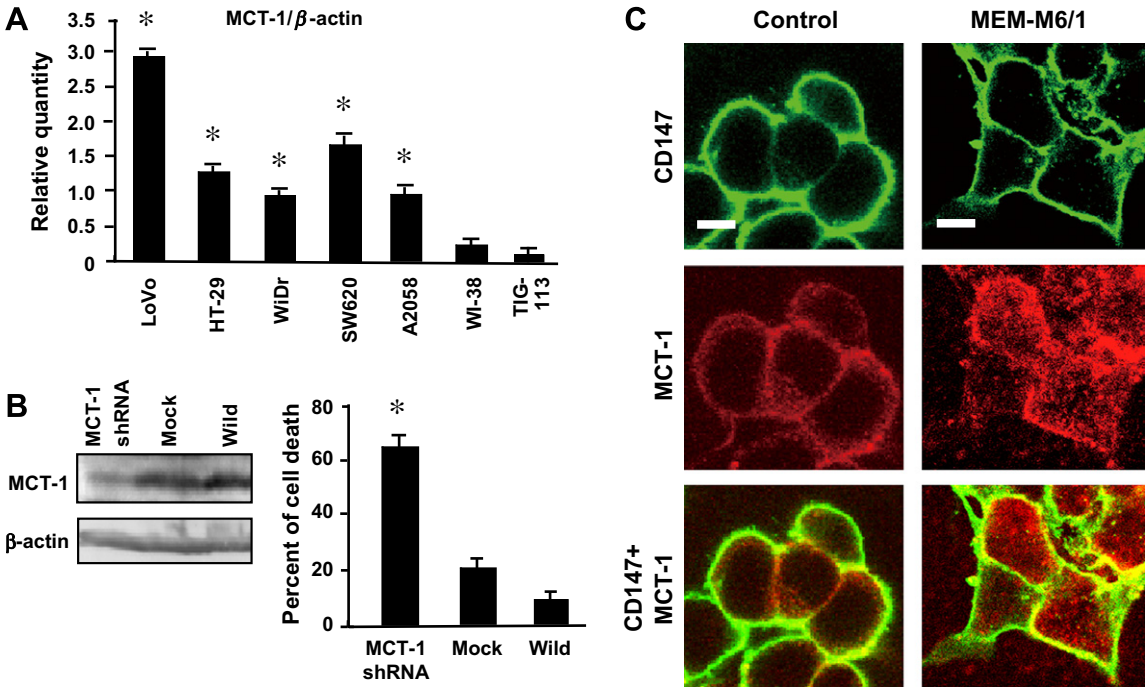


**Fig. 3.** MCT-1 mRNA levels in colon cancer cells, LoVo, HT-29, WiDr, and SW620, A2058 melanoma cells, and normal fibroblasts WI-38 and TIG-113. The levels of MCT-1 mRNA were measured by Real-time PCR and defined as the ratio of MCT-1 mRNA to β-actin mRNA (A). Western blotting of MCT-1 from MCT1 shRNA or control vector (Mock) transfected cells, and Wild (parent) cells is shown in (B left). Percent cell death of these cells after 72 h transfection is shown in (B right). Each value represents mean ± SE from eight measurements in duplicate experiments. $^{*}p < 0.001$ vs. WI-38 and TIG-113 cells (A). $^{*}p < 0.05$ vs. mock-transfected and wild cells (B). Immunofluorescence of LoVo cells after 36 h treated with or without 2.5 μg/ml MEM-M6/1 (C). Bar = 10 μm.

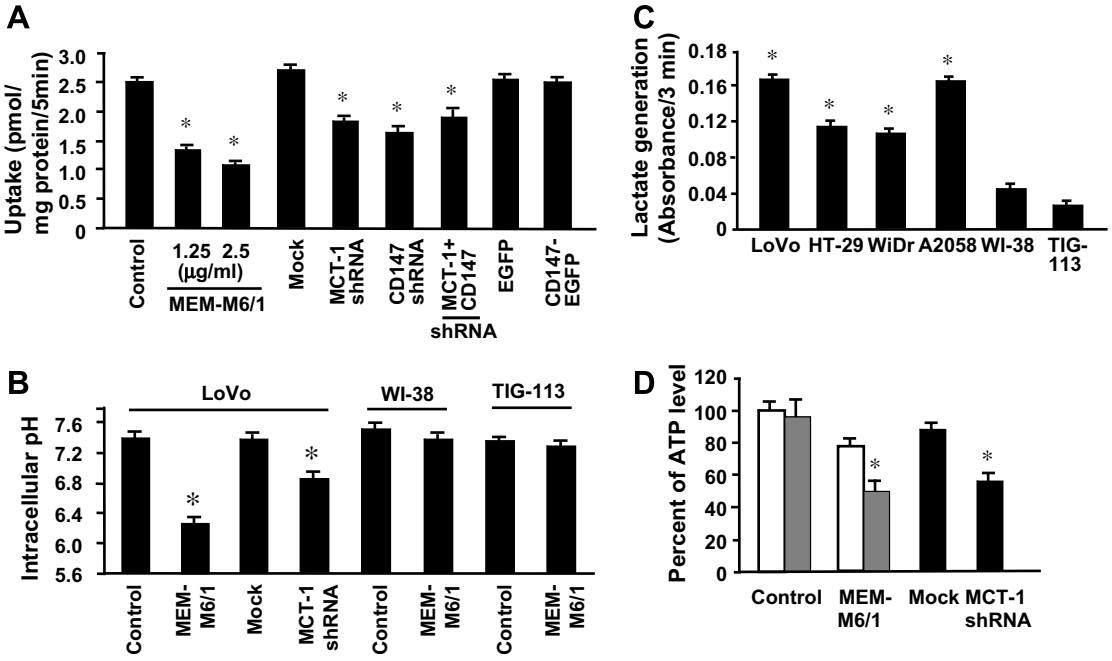


**Fig. 4.** (A) Lactate uptake in LoVo cells, after 48 h treated with or without indicated doses of MEM-M6/1, and in the cells after 48 h transfected with indicated vectors. (B) Intracellular pH in the indicated cells, after 48 h treated with or without 2.5 μg/ml MEM-M6/1. The results from LoVo cells after 48 h transfected with empty or shRNA/MCT-1 vector are also shown in (A) and (B). Each value represents mean ± SE from eight measurements in duplicate experiments. $^{*}p < 0.05$ vs. each control cell. (C) The levels of glycolytic flux in various cancer cell lines and normal fibroblast cell lines. Each value represents mean ± SE from three measurements. $^{*}p < 0.05$ vs. WI-38 and TIG-113 cells. (D) The cellular ATP levels of LoVo cells, after 24 (white column) or 48 (grey column) hours treated with or without 2.5 μg/ml MEM-M6/1. The cellular ATP levels, 48 h after transfection with shRNA/MCT-1 or empty vector (Mock) are also shown in (D). Each value represents mean ± SE from eight measurements. $^{*}p < 0.05$ vs. each control cells.

(Fig. 4A and B, and Supplementary Fig. 5). These effects of MEM-M6/1 on pHi homeostasis were not observed in normal fibroblast cells (Fig. 4B and Supplementary Fig. 5). We further examined the role of CD147 on lactate transport in LoVo cells. In the CD147 knockdown cells, the levels of lactate uptake were decreased as well as MCT-1 knockdown cells, meanwhile it should be noted that

the levels of lactate uptake in double knockdown cells of CD147 and MCT-1 were similar to those of each single knockdown (Fig. 4A). In addition, the CD147 overexpression cells did not increase the levels of lactate uptake (Fig. 4A). These results indicate that MEM-M6/1 inhibited MCT-1 function by blocking formation of CD147/MCT-1 complex.

*MEM-M6/1 induced cell death through impairment of ATP production by glycolysis*

To assess whether induction of cell death by MEM-M6/1 is due to the dependency on glycolysis for ATP production, the glycolytic flux was examined in cancer cells and normal fibroblasts. The glycolytic flux was higher in cancer cells compared to the normal fibroblasts (Fig. 4C), indicating that these cancer cells mainly depended on glycolysis more than normal fibroblasts in ATP production. The levels of cellular ATP rapidly decreased during 48-h culture with MEM-M6/1 or by transfection of MCT-1 shRNA (Fig. 4D). The results were in accordance with the previous report showing that glycolytic inhibition induced cell death due to depletion of ATP in HL-60 cancer cells [21]. Collectively these results indicate that MEM-M6/1-induced cell death occurred through inhibition of glycolysis followed by reduction of intracellular ATP.

## Discussion

Warburg observed that cancer cells frequently exhibit increased glycolysis and depend largely on this metabolic pathway for generation of ATP [1]. In this study, we showed that an anti-CD147 antibody MEM-M6/1 robustly induced cell death in colon cancer cells and melanoma cells but not two normal fibroblasts cell lines (Fig. 1B). The glycolytic flux was enhanced in four of their cancer cells compared to normal fibroblasts (Fig. 4C), suggesting that these cancer cells depend on glycolysis for ATP production and that MEM-M6/1-induced cell death is cancer cell specific. In this regard, targeting of CD147 might be a novel strategy for cancer therapy. However, it is of note that in CD147-knockout mice, half of them die within 1 month after birth and that the surviving adult mutant mice are sterile [22] and suffer from severe defects due to MCTs impairment in the neuronal system [23]. Therefore, inhibition of CD147 causes damage of normal cells in a cell-specific manner.

Various anti-human CD147 mouse monoclonal antibodies (MEM-M6/1-13, AAA6, UM-8D6 and H84) with different epitopes have been generated, and their neutralization effects against CD147 are distinct from each other [24]. UM-8D6 was unable to induce LoVo cell death (data not shown). The epitope for MEM-M6/1 is located in the extracellular N-terminal Ig domain (D1), but the precise amino acid sequence is not known [9]. Thus, the mechanism of impairment of MCT-1 function by MEN-M6/1 is unclear. MEM-M6/1 might inhibit the association between CD147 and MCT-1, although the extracellular domain of the CD147 is reportedly not involved in its interaction with MCTs [6]. Further investigation of the precise interaction between the two molecules is required to elucidate the role of MEN-M6/1 on CD147/MCT-1 interaction.

Most solid tumors contain hypoxic regions, and glycolysis is promoted in hypoxic cells [25]. We observed that glycolysis was enhanced in HT-29 cells under hypoxic conditions, in which MEM-M6/1-induced cell death was quickened (Supplementary Fig. 6). Therefore, cancer cells in hypoxic regions might be effectively impaired by targeting with CD147; indeed, HCT 116 colon cancer cells and Raji cells under hypoxic conditions are reported to be more sensitive to glycolytic inhibition by 3-bromopyruvate (3-BrPA), an inhibitor of hexokinase II [21]. Taken together, anti-CD147 neutralizing antibody, such as MEN-M6/1, can be a novel molecular target of cancer therapy.

## Acknowledgments

We thank Dr. Masaharu Tatsuta (Department of Gastrointestinal Oncology, Osaka Medical Center for Cancer and Cardiovascular Diseases, Osaka Japan) for his encouragement and support.

## Appendix A. Supplementary data

Supplementary data associated with this article can be found, in the online version, at doi:10.1016/j.bbrc.2008.06.122.

## References

[1] O. Warburg, On the origin of cancer cells, Science 123 (1956) 309–314.
[2] D.F. Rolf, G.C. Brown, Cellular energy utilization and molecular origin of standard metabolic rate in mammals, Physiol. Rev. 77 (1997) 731–758.
[3] S.P. Mathupala, P. Parajuli, A.E. Sloan, Silencing of monocarboxylate transporters via small interfering ribonucleic acid inhibits glycolysis and induces cell death in malignant glioma: an in vitro study, Neurosurgery 55 (2004) 1410–1419.
[4] A.P. Halestrap, N.T. Price, The proton-linked monocarboxylate transporter (MCT) family: structure, function and regulation, Biochem. J. 343 (1999) 281–299.
[5] A.A. Deora, N. Philip, J. Hu, D. Bok, E. Rodriguez-Boulan, Mechanisms regulating tissue-specific polarity of monocarboxylate transporters and their chaperone CD147 in kidney and retinal epithelia, Proc. Natl. Acad. Sci. USA 102 (2005) 16245–16250.
[6] P. Kirk, M.C. Wilson, C. Heddle, M.H. Brown, A.N. Barclay, A.P. Halestrap, CD147 is tightly associated with lactate transporters MCT1 and MCT4 and facilitates their cell surface expression, EMBO J. 19 (2000) 3896–3904.
[7] S.M. Gallagher, J.J. Castorino, D. Wang, N.J. Philp, Monocarboxylate transporter 4 regulates maturation and trafficking of CD147 to the plasma membrane in the metastatic breast cancer cell line MDA-MB-231, Cancer Res. 67 (2007) 4182–4189.
[8] C. Biswas, Y. Zhang, R. DeCastro, H. Guo, T. Nakamura, H. Kataoka, K. Nabeshima, The human tumor cell-derived collagenase stimulatory factor (renamed EMMPRIN) is a member of the immunoglobulin superfamily, Cancer Res. 55 (1995) 434–439.
[9] C. Koch, G. Staffler, R. Huttinger, I. Hilgert, E. Prager, J. Cerny, P. Steinlein, O. Majdic, V. Horejsi, H. Stockinger, T cell activation-associated epitopes of CD147 in regulation of the T cell response, and their definition by antibody affinity and antigen density, Int. Immunol. 11 (1999) 777–786.
[10] X. Chen, J. Lin, T. Kanekura, J. Su, W. Lin, H. Xie, Y. Wu, J. Li, M. Chen, J. Chang, A small interfering CD147-targeting RNA inhibited the proliferation, invasiveness, and metastatic activity of malignant melanoma, Cancer Res. 66 (2006) 11323–11330.
[11] E.A. Marieb, A. Zoltan-Jones, R. Li, S. Misra, S. Ghatak, J. Cao, S. Zucker, B.P. Toole, Emmprin promotes anchorage-independent growth in human mammary carcinoma cells by stimulating hyaluronan production, Cancer Res. 64 (2004) 1229–1232.
[12] R. Li, L. Huang, H. Guo, B.P. Toole, Basigin (murine EMMPRIN) stimulates matrix metalloproteinase production by fibroblasts, J. Cell. Physiol. 186 (2001) 371–379.
[13] S. Caudroy, M. Polette, B. Nawrocki-Raby, J. Cao, B.P. Toole, S. Zucker, P. Birembaut, EMMPRIN-mediated MMP regulation in tumor and endothelial cells, Clin. Exp. Metastasis 19 (2002) 697–702.
[14] J. Sun, M.E. Hemler, Regulation of MMP-1 and MMP-2 production through CD147/extracellular matrix metalloproteinase inducer interactions, Cancer Res. 61 (2001) 2276–2281.
[15] Y. Tang, M.T. Nakada, P. Kesavan, F. McCabe, H. Millar, P. Rafferty, P. Bugelski, L. Yan, Extracellular matrix metalloproteinase inducer stimulates tumor angiogenesis by elevating vascular endothelial cell growth factor and matrix metalloproteinases, Cancer Res. 65 (2005) 3193–3199.
[16] D. Xu, M.E. Hemler, Metabolic activation-related CD147-CD98 complex, Mol. Cell. Proteomics 4 (2005) 1061–1071.
[17] M. Baba, K. Itoh, M. Tatsuta, Glycine-extended gastrin induces matrix metalloproteinase-1- and -3-mediated invasion of human colon cancer cells through type I collagen gel and matrigel, Int. J. Cancer 111 (2004) 23–31.
[18] M. Kobayashi, I. Fujita, S. Itagaki, T. Hirano, K. Iseki, Transport mechanism for L-lactic acid in human myocytes using human prototypic embryonal rhabdomyosarcoma cell line (RD cells), Biol. Pharm. Bull. 28 (2005) 1197–1201.
[19] P. Frank, N. Petitipain, M. Cherlet, M. Dardennes, F. Maachi, B. Schutz, L. Poisson, P. Nabet, Measurement of intracellular pH in cultured cells by flow cytometry with BCECF-AM, J. Biotech. 46 (1996) 187–195.
[20] A. Marin-Hernandez, S. Rodriguez-Enriquez, P.A. Vital-Gonzalez, F.L. Flores-Rodriguez, M. Macias-Silva, M. Sosa-Garrocho, R. Moreno-Sanchez,

Determining and understanding the control of glycolysis in fast-growth tumor cells, FEBS J. 273 (2006) 1975–1988.
[21] R.H. Xu, H. Pelicano, Y. Zhou, J.S. Carew, L. Feng, K.N. Bhalla, M.J. Keating, P. Huang, Inhibition of glycolysis in cancer cells: a novel strategy to overcome drug resistance associated with mitochondrial respiratory defect and hypoxia, Cancer Res. 65 (2005) 613–621.
[22] T. Igakura, K. Kadomatsu, T. Kaname, H. Muramatsu, Q.-W. Fan, T. Miyauchi, Y. Toyama, N. Kuno, S. Yuasa, M. Takahashi, T. Senda, O. Taguchi, K. Arimura, T. Muramatsu, A null mutation in basigin, an immunoglobulin superfamily member, indicates its important roles in peri-implantation development and spermatogenesis, Dev. Biol. 194 (1998) 152–165.
[23] N.J. Philip, J.D. Ochrietor, C. Rudoy, T. Muramatsu, P.J. Linser, Loss of MCT1, MCT3, and MCT4 expression in the retinal pigment epithelium and neural retina of the 5A11/basigin-null mouse, Invest. Ophthalmol. Vis. Sci. 44 (2003) 1305–1311.
[24] E.M. Schiavone, V. Tortora, I. Armetta, P. Bontempo, M.R. Mosti, L. Pezone, E. Nola, G.A. Puca, C. Vacca, A.M. Molinari, CD147 Workshop: expression, modulation, and involvement in homotypic aggregation and adhesion to matrix of molecules recognized by monoclonal antibodies to CD147 on breast cancer cell lines, Leucocyte Typing 4 (1997) 784–785.
[25] G.L. Semenza, P.H. Roth, H.M. Fang, G.L. Wang, Transcriptional regulation of genes encoding glycolytic enzymes by hypoxia-inducible factor 1, J. Biol. Chem. 269 (1994) 23757–23763.
[26] W. Tang, S.B. Chang, M.E. Hemler, Links between CD147 function, glycosylation, and caveolin-1, Mol. Biol. Cell 15 (2004) 4043–4050.